

Intrinsic deep hole trap levels in Cu_2O with self-consistent repulsive Coulomb energy

B. Huang*

(Dated: March 30, 2025)

The large error of the DFT+U method on full-filled shell metal oxides is due to the residue of self-energy from the localized d orbitals of cations and p orbitals of the anions. U parameters are self-consistently found to achieve the analytical self-energy cancellation. The improved band structures based on relaxed lattices of Cu_2O are shown based on minimization of self-energy error. The experimentally reported intrinsic p-type trap levels are contributed by both Cu-vacancy and the O-interstitial defects in Cu_2O . The latter defect has the lowest formation energy but contributes a deep hole trap level while the Cu-vacancy has higher energy cost but acting as a shallow acceptor. Both present single-particle levels spread over nearby the valence band edge, consistent to the trend of defects transition levels. By this calculation approach, we also elucidated the entanglement of strong p-d orbital coupling to unravel the screened Coulomb potential of fully filled shells.

PACS numbers: 71.20.Nr, 71.55.-i

Cuprous oxide (Cu_2O) is a direct gap semiconducting oxide with full/nearly filled shell for Cu. It has been regarded as one of the most promising candidate of photovoltaic cells. It is also a prototype materials of “invisible electronic devices” derived from $CuMO_2$ (M=Al, Ga, In, Cr, etc.) with wide energy range of p-type doping limit determined by intrinsic defects [1]. Using the DFT+U method on these materials, we can rapidly determine electronic structures of the atomic models [2]. Furthermore, a linear response method can be used to obtain a localized partially filled model; however, it is difficult to obtain the correct U parameter estimate for the $3d^{10}$ configuration. The electron wavefunctions of $3d^{10}$ are constrained with strict boundary conditions. Therefore, the perturbation becomes extremely small if a small Lagrange multiplier is used to perturb the fully filled localized orbital. The inverse of this small difference tends to be a singularity (e.g., $1/\chi$ with $\chi \rightarrow 0$). Thus, the simple U parameter estimation through the small perturbation inverse using linear response becomes unphysical. Therefore, the first issue is start from the $3d^{10}$ orbital energy.

More unusually, an interesting scenario happens in ZnO also with $3d^{10}$ configuration for Zn^{2+} . The electronic structures and lattice relaxation exhibit a strong correlation for zincblend, rocksalt, and wurtzite phases of ZnO. Ma et al has empirically tuned U parameters for 3d orbitals of Zn and 2p orbitals of O respectively, and shown this effect [3] in terms of band structure, lattice geometry, and native defect levels. And this effect occurs regardless the local atomic coordination, which hints an intrinsic feature. However, we need to understand the reason through the theory level of self-consistent determination p-d orbital entanglement.

On the other hand, the actual 3d orbital occupations between cubic Cu_2O and monoclinic CuO in antiferromagnetic phase are still unknown by DFT+U. There has

been a long debate between $3d^{10}$ and $3d^9$ for ground state Cu_2O and CuO. The band structure calculations of Cu_2O by DFT+U always underestimate the band gap due to strong p-d orbital entanglement. This directly leads to incorrect density of states for p and d orbitals known from Sieberer et al [4] where the p and d orbitals levels were shown to be mixed at valence band maximum. Robertson et al [5] has given accurate band structure and optical property of Cu_2O , and confirmed that the 2p orbital of O is in fact lower than the 3d orbital of Cu and 3d levels contribute the VBM. Hybrid functional has shown coherent orbital energies of the band structure but left a potential error for band gap by Heinemann et al [6] and Robertson et al [7].

The estimation of the Coulomb repulsive potential in DFT+U is tried by Cococcioni [8, 9] but fails in predicting the energy for fully occupied orbitals. This arises because the pristine Janak theorem that linear response relies on omitted the spurious Coulomb self-energy of the semicore orbitals. This amplifies the error of self-energy term when applying U on such orbitals for projecting the semicore states out. Regarding the Coulomb self-energy correction of Perdew and Zunger [10], the strict conditional of correction has been updated into Janak equation [11] as following forms.

$$\begin{cases} \frac{\delta \bar{E}}{\delta n_i} = (\epsilon_i)_{cation} + \Sigma_{cation} \\ \frac{\delta \bar{E}}{\delta n_j} = (\epsilon_j)_{anion} + \Sigma_{anion} \end{cases} \quad (1)$$

The i and j denotes the i th cation and j th anion respectively. The $(\epsilon_i)_{cation}$ and $(\epsilon_j)_{anion}$ are orbital eigenvalues for lining up the band structures. The Σ_{cation} and Σ_{anion} are self-energies induced by semicore states of cations and anions, to be annihilated ideally fowling the condition of $\mathbf{U}[n_{\alpha\sigma}] + E_{XC}[n_{\alpha\sigma}, 0] = 0$, by Perdew and Zunger [10]. By a self-consistent linear response procedure, the U parameters assigned to both cations and anions are reliably obtained [12]. FIG. 1 shows how the self-energy to be counteracted in fully occupied shell of cations. We choose the non-linear core-corrected norm-conserving pseudopotentials for both the cation and anion elements [2]. The norm-conserving pseudopotentials

* Department of Physics and Materials Science, City University of Hong Kong, Kowloon, Hong Kong
Email: bolhuang@cityu.edu.hk

reflect the all-electron behavior for the outer shell valence electrons with $|\mathbf{S} - \mathbf{matrix}| = 1$ compared with ultrasoft pseudopotentials [13, 14].

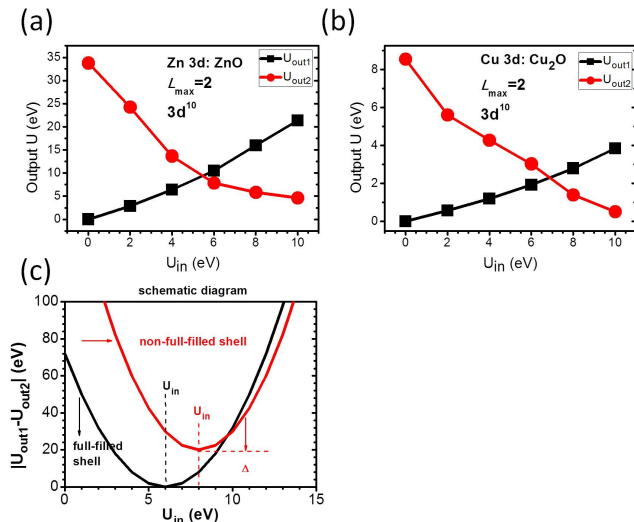


FIG. 1. Self-consistently obtained U_{out1} and U_{out2} for fully occupied orbitals from (a) ZnO, (b) Cu_2O . The cross-over feature of fully occupied shell denotes the $|U_{out1} - U_{out2}| = 0$, shown in (c).

The origin of the intrinsic p-type conductivity in Cu_2O has been under investigation for a long time. Experiment reported the two acceptor-like levels with two different trends of densities variation with increasing oxygen chemical potential [15]. Scanlon et al. proposed that the intrinsic p-type conductivity in Cu_2O is attributed to Cu binding to Cu-vacancy with tetrahedral coordinate (V_{Cu}^{split}) using a HSE study and contributes to a deep localized state [16, 17]. However, Isseroff et al. [18] used the same HSE method and determined that the V_{Cu}^{split} is approximately 0.5 eV higher than normal V_{Cu} . This is attributed to oxygen hole levels that are not well counteracted. Both Raebiger et al [19] and Soon et al [20] reported the O-interstitials act as deep hole trap levels, but with higher formation energy than the Cu-vacancy which gives shallower hole trap levels. This requires to confirm by accurate band gap and oxygen hole levels. However, recent experiment [15] shows that the concentration of deeper trap level is higher at high temperature (> 750 K) or with relatively wide range of oxygen chemical potential.

We hold the opinion that, the O-interstitial defect in fact has the same chemical potential trend as the Cu-vacancy, and is the result of the deep hole trap level. Furthermore, the total energy of monoclinic CuO with corrected Hubbard U is difficult to determine because it provides the lower limit of the Cu chemical potential for the defect formation energy calculations in Cu_2O .

FIG. 2 presents the variation behaviors of d and p orbitals for the $3d^{10}$ -based compounds. The p orbitals perturbed by linear response also have a crossover behavior

similar to that of the d^{10} orbitals. The strong p-d coupling leads to a large portion of charge transfer from adjacent d orbitals to the p orbitals of valence electrons of the anion elements. This elucidates the validation for the total energy with related to the occupation number of electron system [21–25].

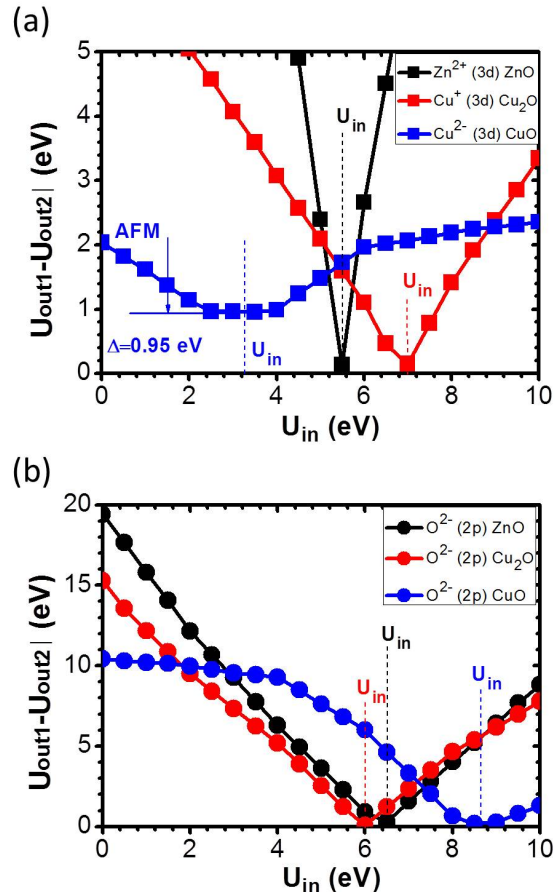


FIG. 2. The $|U_{out1} - U_{out2}|$ vs. U_{in} behaviors of bulk wurtzite ZnO, bulk CuO in the AFM phase and bulk Cu_2O structures with (a) d and (b) p localized electronic orbitals. (AFM: anti-ferromagnetic). Cu^{2+} in CuO cannot achieve the full filled shell with a rigid Δ shift (a).

According to FIG. 2, we obtained a d-orbital Hubbard correction of 6.8 eV for Cu and normalized 12 eV for O 2p orbitals. The twice-large Hubbard correction for the 2p orbitals of O occurs because each O site experiences two Cu-localized electron perturbations in the linear response calculations. As shown in FIG. 2, Cu presents the fully filled shell feature in the Cu_2O system as it touches the 0 eV level. However, each perturbation of the d-electrons shared with one O site. Therefore, this is different from other ordinary coordinated metal oxides because metal atoms typically have a larger coordination number when bound to O. Therefore, Cu_2O has a reversed CaF_2 structure because O occupies the Ca site, whereas Cu occupies the F site. The band structures of Cu_2O and CuO in the

AFM phase are shown in FIG. 3 (a) and (b).

The experimentally determined acceptor-like trap states are two states that are $E_V+0.25$ and $E_V+0.45$ eV [15]. However, because the oxygen flux was increased in those experiments, one of the densities of the trap states increased, whereas the other decreased to a lower density. This suggests that the O-related intrinsic defects play a significant role in providing acceptor-like trap levels near the VBM, and form unfavorable O-O homopolar bond under high O-concentration. However, as stated previously, this requires an accurate description of the localized hole states induced by the O-2p orbitals [2].

As shown in Table 1, our method produces consistent lattice parameters and electronic band gaps of Cu_2O , which is experimentally determined to be 2.17 eV. Isseroff et al. consider whether the V_{Cu}^{split} has a lower formation energy than the simple Cu-vacancy [18]. Our data are consistent with Scanlon et al [16, 17], because the neutral V_{Cu}^{split} is approximately 0.8 eV lower than the V_{Cu}^{simple} with help of local lattice reconstructions. This indicates that the corrected O-2p orbital energies improve the defect formation studies. One may argue that the Hubbard U parameter correction for O-2p orbitals is too high, with a magnitude of 12 eV. However, the formation energies of O-interstitial defects in tetrahedral and octahedral (I_O^{tet} and I_O^{oct}) have similar values as the data provided by HSE, with an HF interaction percentage of 0.275, in the work of Scanlon et al [16, 17]. Thus, the O-2p orbital correction, in terms of Hubbard U, does not affect either the defect formation energies or thermal dynamic transition levels in different charges.

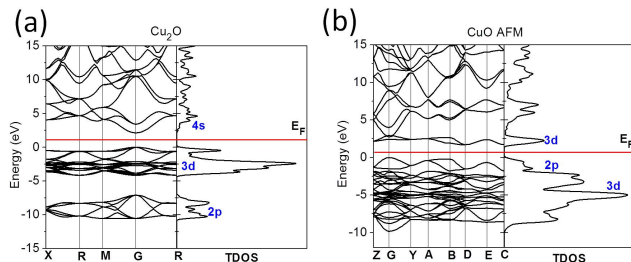


FIG. 3. (a) The band structure and TDOS of (a) Cu_2O and (b) CuO in the AFM phase. (c) A summary of the formation energies of the intrinsic defects in Cu_2O under O-rich and O-poor limit. (d) The localized single-particle level within the band gap of Cu_2O .

As shown in FIG. 4 (a), the contribution of the p-type intrinsic conductivity of Cu_2O does not originate from V_{Cu}^{split} . The formation energies of the V_{Cu} and simple V_{Cu} are similar to the work of Scanlon et al, and the V_{Cu}^{split} is approximately 0.6 eV lower than the simple V_{Cu} . This confirms that the Cu atom favors a flexible structural relaxation to a more stable tetrahedral coordination. However, this is not the lowest-energy defect, and neither is the oxygen vacancy (V_O). Instead, the lowest-energy defect is the oxygen interstitials (I_O). The

experiments show that Cu_2O is stabilized in the high-temperature condition because it follows the following reaction process from CuO : $4CuO \rightarrow 2Cu_2O + O_2 \uparrow$. The Cu_2O structure has many hollow channels through which oxygen can diffuse. The excess O is trapped in this channel and induces localized states to capture electrons. The tetrahedral IO (I_O^{tet}) has an even lower formation energy compared with V_{Cu}^{split} . But octahedral IO (I_O^{oct}) determines the upper bound of the Fermi level for extrinsic doping where causes the defect formation spontaneously. The upper doping limit energy is about $E_V+1.8$ eV referring to the 0 eV of formation energy that is nearly constant from O-poor to O-rich potential limits, shown in FIG. 4 (a).

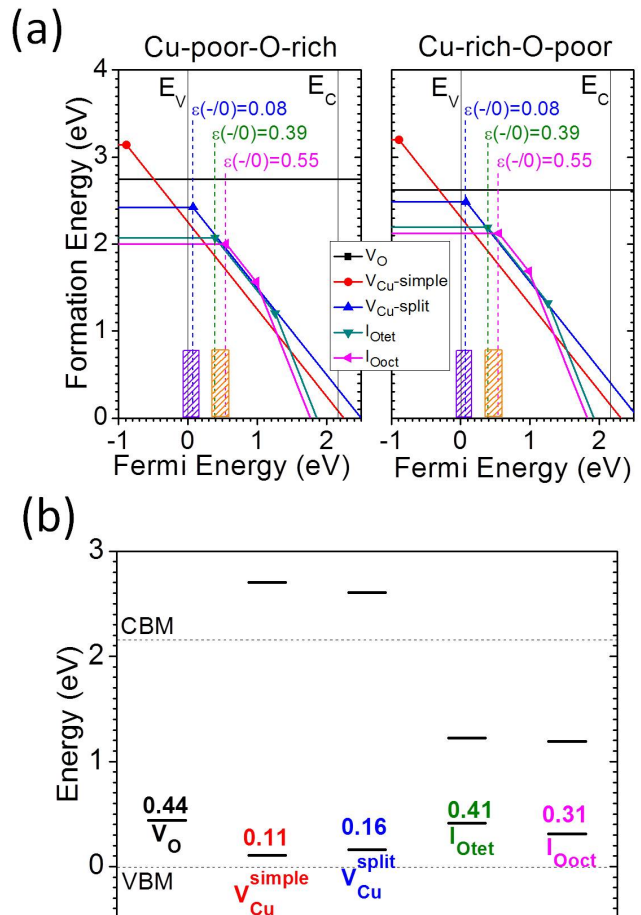


FIG. 4. (a) A summary of the formation energies of the intrinsic defects in Cu_2O under O-rich and O-poor limit. (b) The localized single-particle level within the band gap of Cu_2O .

The single-particle levels shown in FIG. 4 (b) demonstrate that V_{Cu}^{split} provides deep localized hole trap states next to the conduction band minimum (CBM), which has a d-orbital feature. The simple V_{Cu} has a localized state that is 0.4 eV higher than the VBM. I_O^{tet} has two localized states that are 0.2 and 0.5 eV higher than the VBM. This is similar to the experimental observations, where the trap states have been reported to be

0.25 and 0.45 eV higher than the VBM [15]. The formation energy of I_O^{tet} is approximately 0.3 eV lower than the V_{Cu}^{split} . The electrical transition levels of (-/0) for V_{Cu}^{split} and I_O^{tet} are $E_V+0.08$ and $E_V+0.39$ that corresponds to the intrinsic p-type behavior. Therefore, the defect formation energies and electronic properties are determined based on the well-counteracted self-interaction, which is induced by the spurious self-energy of the localized orbitals. The experimentally reported intrinsic p-type conduction was found to be contributed by both V_{Cu}^{split} and the O-interstitial intrinsic defects in Cu_2O . Both have similar formation energies in the range from (0/-1) to (-

1/-2) transition states, with two single-particle trapping levels higher than the VBM.

Finally, the description of localized hole levels using DFT is the complicated issue for metal oxides. For the metal vacancy or anion interstitial site, the induced holes (removal of electrons) are often localized at the p- π orbitals of nearby O-sites, which denote levels near the valence band maximum (VBM). To accurately calculate these hole-induced levels, the Hubbard U parameter is used to correct the O-2p orbital energies in metal oxides. These orbital energies have been proven to significantly improve their single-particle levels in the band gap [2, 26–28].

-
- [1] J. Robertson and S. J. Clark, Phys. Rev. B **83**, 075205 (2011).
- [2] B. Huang, R. Gillen, and J. Robertson, The Journal of Physical Chemistry C **118**, 24248 (2014).
- [3] X. Ma, Y. Wu, Y. Lv, and Y. Zhu, The Journal of Physical Chemistry C **117**, 26029 (2013).
- [4] M. Sieberer, J. Redinger, and P. Mohn, Phys. Rev. B **75**, 035203 (2007).
- [5] J. Robertson, Phys. Rev. B **28**, 3378 (1983).
- [6] M. Heinemann, B. Eifert, and C. Heiliger, Phys. Rev. B **87**, 115111 (2013).
- [7] J. Robertson and B. Felebratti, Chapter 1, Handbook of Transparent Conductors (2011).
- [8] M. Cococcioni and S. de Gironcoli, Phys. Rev. B **71**, 035105 (2005).
- [9] H. J. Kulik, M. Cococcioni, D. A. Scherlis, and N. Marzari, Phys. Rev. Lett. **97**, 103001 (2006).
- [10] J. P. Perdew and A. Zunger, Phys. Rev. B **23**, 5048 (1981).
- [11] J. F. Janak, Phys. Rev. B **18**, 7165 (1978).
- [12] B. Huang, arXiv e-prints (2015), 1507.05040.
- [13] P. Hasnip and C. Pickard, Computer Physics Communications **174**, 24 (2006).
- [14] K. Laasonen, A. Pasquarello, R. Car, C. Lee, and D. Vanderbilt, Phys. Rev. B **47**, 10142 (1993).
- [15] G. K. Paul, Y. Nawa, H. Sato, T. Sakurai, and K. Akimoto, Applied Physics Letters **88**, 141901 (2006).
- [16] D. O. Scanlon, B. J. Morgan, G. W. Watson, and A. Walsh, Phys. Rev. Lett. **103**, 096405 (2009).
- [17] D. O. Scanlon and G. W. Watson, Phys. Rev. Lett. **106**, 186403 (2011).
- [18] L. Y. Isseroff and E. A. Carter, Chemistry of Materials **25**, 253 (2013).
- [19] H. Raebiger, S. Lany, and A. Zunger, Phys. Rev. B **76**, 045209 (2007).
- [20] A. Soon, X.-Y. Cui, B. Delley, S.-H. Wei, and C. Stampfl, Phys. Rev. B **79**, 035205 (2009).
- [21] J. P. Perdew, A. Ruzsinszky, G. I. Csonka, O. A. Vydrov, G. E. Scuseria, V. N. Staroverov, and J. Tao, Phys. Rev. A **76**, 040501 (2007).
- [22] P. Mori-Sánchez, A. J. Cohen, and W. Yang, Phys. Rev. Lett. **100**, 146401 (2008).
- [23] J. P. Perdew, R. G. Parr, M. Levy, and J. L. Balduz, Phys. Rev. Lett. **49**, 1691 (1982).
- [24] S. Lany and A. Zunger, Phys. Rev. B **80**, 085202 (2009).
- [25] S. Lany and A. Zunger, Phys. Rev. B **81**, 205209 (2010).
- [26] R. Pentcheva and W. E. Pickett, Phys. Rev. B **74**, 035112 (2006).
- [27] A. K. McMahan, R. M. Martin, and S. Satpathy, Phys. Rev. B **38**, 6650 (1988).
- [28] O. Volnianska, T. Zakrzewski, and P. Boguslawski, The Journal of Chemical Physics **141**, 114703 (2014).
- [29] M. Nolan and S. D. Elliott, Phys. Chem. Chem. Phys. **8**, 5350 (2006).
- [30] D. R. Lide, (CRC Press), Boca Raton, FL (2011).

TABLE I. Table 1. Summary of the lattice parameters, formation enthalpies of Cu₂O and CuO (AFM), defect formation energies in (Cu-rich/O-poor), single-particle levels, and transition levels. [16, 18–20, 29, 30]

		PBE [19]	GGA [20]	PBE+ U [29]	PBE+ U [18]	HSE (0.275) [18]	HSE (0.275) [16]	This work	Exp [30]
	Latt. (Å)	4.31	4.32					4.28	4.27
	E _g	0.43	0.46	0.4		2.12	2.12	2.16	2.17
ΔH_f	Cu ₂ O		-1.24		-1.64	-1.62	-1.59	-1.79	-1.75
	CuO				-1.21	-1.44	-1.46	-1.74	-1.63
ΔH_f (D, 0) (eV)	V _{Cu} ^{simple}	0.70	0.47	0.41	1.10	1.34	1.15	3.20	
	V _{Cu} ^{split}	1.00	0.78	0.47	1.28	1.58	1.14	2.48	
	I _O ^{oct}	1.80	1.90				1.94	2.12	
	I _O ^{tet}	1.30	1.47				1.87	2.19	
	V _O	0.80	0.90				1.20	2.62	
SPL (eV)	V _{Cu} ^{simple}	0.00	0	0.00			0.52	0.11	
	V _{Cu} ^{split}					0.57	1.12	0.16	
	I _O ^{oct}						1.14	0.31	
	I _O ^{tet}						1.05	0.41	
	V _O							0.44	
(-/0) (eV)	V _{Cu} ^{simple}	0.28	0.18				0.23	-0.89	
	V _{Cu} ^{split}	0.29	0.20				0.47	0.08	
	I _O ^{oct}	0.66	0.45				1.08	0.55	
	I _O ^{tet}	0.78	0.65				1.27	0.39	